Animal Nutrition 8 (2022) 91–101

Contents lists available at ScienceDirect

Animal Nutrition

journal homepage: http://www.keaipublishing.com/en/journals/aninu/

Original Research Article

Nutritional stimulation by in-ovo feeding modulates cellular proliferation and differentiation in the small intestinal epithelium of chicks

Naama Reicher [a], Tal Melkman-Zehavi [a], Jonathan Dayan [a], Eric A. Wong [b], Zehava Uni [a, *]

[a] Department of Animal Science, The Robert H. Smith, Faculty of Agriculture, Food and Environment, The Hebrew University of Jerusalem, Rehovot 76100, Israel
[b] Department of Animal and Poultry Sciences, Virginia Tech, Blacksburg, VA 24061, USA

ARTICLE INFO

Article history:
Received 4 February 2021
Received in revised form
24 May 2021
Accepted 10 June 2021
Available online 23 September 2021

Keywords:
Chick
Intestinal development
Proliferation
Differentiation
Multipotent cells
In-ovo feeding

ABSTRACT

Nutritional stimulation of the developing small intestine of chick embryos can be conducted by in-ovo feeding (IOF). We hypothesized that IOF of glutamine and leucine can enhance small intestinal development by promoting proliferation and differentiation of multipotent small intestinal epithelial cells. Broiler embryos ($n = 128$) were subject to IOF of glutamine (IOF-Gln), leucine (IOF-Leu), NaCl (IOF-NaCl) or no injection (control) at embryonic d 17 (E 17). Multipotent, progenitor and differentiated cells were located and quantified in the small intestinal epithelium between E 17 and d 7 after hatch (D 7) in all treatment groups by immunofluorescence of SRY-box transcription factor 9 (Sox9) and proliferating cell nuclear antigen (PCNA), in-situ hybridization of leucine-rich repeat containing G-protein coupled receptor 5 (Lgr5) and peptide transporter 1 (PepT1) and histochemical goblet cell staining. The effects of IOF treatments at E 19 (48 h post-IOF), in comparison to control embryos, were as follows: total cell counts increased by 40%, 33% and 19%, and multipotent cell counts increased by 52%, 50% and 38%, in IOF-Gln, IOF-Leu and IOF-NaCl embryos, respectively. Only IOF-Gln embryos exhibited a significance, 36% increase in progenitor cell counts. All IOF treatments shifted Lgr5+ stem cell localizations to villus bottoms. The differentiated, PepT1+ region of the villi was 1.9 and 1.3-fold longer in IOF-Gln and IOF-Leu embryos, respectively, while goblet cell densities decreased by 20% in IOF-Gln embryos. Post−hatch, crypt and villi epithelial cell counts were significantly higher IOF-Gln chicks, compared to control chicks ($P < 0.05$). We conclude IOF of glutamine stimulates small intestinal maturation and functionality during the peri-hatch period by promoting multipotent cell proliferation and differentiation, resulting in enhanced compartmentalization of multipotent and differentiated cell niches and expansions of the absorptive surface area.

1. Introduction

The mucosal lining of the small intestine is a highly functional epithelium comprised of absorptive, secretive and sensory cells, which are constantly renewed by multipotent intestinal stem cells (ISC). ISC reside within crypts, and constantly proliferate for self-renewal and generation of progenitor cells, which differentiate into the functional cells that line lumen-facing villi (Carulli et al., 2014; Potten and Loeffler, 1990). Compartmentalization of the multipotent and differentiated regions of the small intestine epithelium occur during villi formation, through a polarized mesenchymal bone morphogenetic protein (BMP) signaling gradient which limits all proliferative, Wnt responsive ISC to the bottom regions of the developing villi. These regions develop into crypts as the small intestine matures, while villi become exclusively populated by differentiated cells (Carulli et al., 2014; Haramis et al., 2004; He et al., 2004). In chicken embryos (*Gallus gallus*), villus

* Corresponding author.
E-mail address: zehava.uni@mail.huji.ac.il (Z. Uni).
Peer review under responsibility of Chinese Association of Animal Science and Veterinary Medicine.

Production and Hosting by Elsevier on behalf of KeAi

https://doi.org/10.1016/j.aninu.2021.06.010

formation occurs at the 15th d of embryonic development (embryonic d 15, E 15), and crypts develop at E 21 (day of hatch, DOH) (Shyer et al., 2013; Uni et al., 2000, 2003a). Post–hatch, initial feeding stimulates the completion of small intestinal maturation through expansions of the crypt and villus epithelium, mediation of cellular proliferation and differentiation and activation of nutrient transporters, digestive enzymes and mucin secretion (Geyra et al., 2001a, 2001b; Reicher et al., 2020; Uni et al., 2003a, 2003b).

Small intestinal development can also be enhanced prior to hatch by nutritional stimulation, through in-ovo feeding (IOF). IOF is a method for supplying nutrients to the small intestine of chicken embryos by injecting their amniotic fluid with a formulated nutrient solution at E 17, prior to amniotic ingestion, which occurs up until DOH (Hamilton, 1952; Romanoff, 1960; Uni and Ferket, 2003). Various studies showed that IOF of specific nutrients enhanced peri-hatch intestinal development and functionality by expanding villi and crypt dimensions and increasing nutrient digestion and absorption capacities (Cheled-Shoval et al., 2011; Dai et al., 2020; Foye et al., 2007; Gao et al., 2017; Kadam et al., 2013; Tako et al., 2004; Wang et al., 2020).

However, no study to date has examined the effects of in-ovo administered nutrients on the dynamics of cellular multipotency, proliferation and differentiation in the small intestinal epithelium of peri-hatch chicks. Evaluating the capacity of IOF for modulating the multipotent and differentiated compartments of the developing small intestine will provide important tools for understanding the link between primary nutritional stimulation and cellular characteristics of the small intestinal epithelium.

In this study, we examined the effects of in-ovo administration of glutamine and leucine on the localizations and proportions of multipotent, progenitor and differentiated cells in the small intestinal epithelium of peri-hatch chicks. Glutamine and leucine were chosen for this study based on their well-documented stimulatory effects on small intestinal epithelial cell proliferation through mitogen-activated protein kinase (MAPK) and mechanistic target of rapamycin (mTOR) signaling pathways (Rhoads et al., 1997; Rhoads and Wu, 2009; Yi et al., 2015), which result in improved small intestine morphology in various animal models, including humans (Coëffier et al., 2011), pigs (Domeneghini et al., 2006; Sun et al., 2015) and chicken Bartell and Batal, 2007; Chang et al., 2015).

Visualizing the pre-hatch small intestinal epithelium, we distinguished between proliferative multipotent cells, which co-expressed proliferating cell nuclear antigen (PCNA) (Kubben et al., 1994) and SRY-box transcription factor 9 (Sox9), a marker for Wnt-responsive intestinal multipotent cells (Blache et al., 2004), and proliferating progenitor cells located above them, which were PCNA-positive, but did not express Sox9. The effects of IOF on the quantities and percentages of these cells were evaluated 48 h post nutrient administration, as well as at DOH, d 1 post-hatch (D 1), D 3 and D 7. We further examined the effects of IOF on small intestinal epithelial development by determining the extent of compartmentalization of stem and differentiated cells within the peri-hatch small intestinal epithelium by in-situ expression of stem cell marker leucine-rich repeat containing G-protein coupled receptor 5 (Lgr5) (Barker et al., 2007), absorptive cell marker SLC15A1/peptide transporter 1 (PepT1) (Fei et al., 2000) and goblet cell mucin staining.

2. Materials and methods

2.1. Incubation, in-ovo feeding and housing

Fertile broiler eggs (Cobb 500, $n = 150$) were obtained from a commercial hatchery (Brown Ltd., Hod-Hasharon, Israel) at day of lay and incubated in a Petersime hatcher at the Faculty of Agriculture of the Hebrew University, under standard conditions (37.8 °C, 60% relative humidity). Egg viability was examined by candling at the 14th d of incubation (E 14) and unviable eggs were discarded. At E 17, eggs were divided into 4 treatment groups ($n = 32$ each) of equal weights (64.5 ± 4.1 g) for IOF procedures. All eggs were placed at room temperature (RT) during IOF procedures and disinfected by spraying of 75% ethanol. Intra-amniotic administration of 0.6 mL sterile nutrient solutions, using a 21-gauge needle, was conducted as described in previous studies (Foye et al., 2007; Uni and Ferket, 2003; Yair et al., 2015), in 3 groups, while eggs of the control group were not injected. Nutrient solutions used were 1) 1% (wt/vol) L-glutamine (Sigma Aldrich, Rehovot, Israel) in 0.4% NaCl (IOF-Gln); 2), 1% (wt/vol) L-leucine (Sigma Aldrich, Rehovot, Israel) in 0.4% NaCl (IOF-Leu); 3) 0.75% NaCl as an injected control (IOFNaCl). Concentrations in the IOF-Gln and IOF-NaCl groups were chosen according to previous studies of in-ovo administrations of amino acids (Dai et al., 2020; Gao et al., 2017). NaCl concentrations in all IOF groups were adjusted for optimal osmolarity of 160 to 180 mOsmol/L and pH of 5.4 to 5.9. Therefore, the IOF-NaCl was injected with a higher concentration of NaCl, compared to the IOF-Gln and IOF-Leu groups.

After IOF procedures, eggs were sprayed again with 75% ethanol and placed back into the hatchery, in hatching trays. Hatching window was monitored from E 20 to E 21 and there were no significant differences between treatment groups. Hatchability was 95%, 96%, 96% and 92% in the control, IOF-NaCl, IOF-Leu and IOF-Gln groups, respectively. Chicks that hatched between E 20.5 and E 21 were marked according to their treatment group and transferred to brooder facilities at the Faculty of Agriculture of the Hebrew University. All groups were given immediate, free access to water and commercial starter feed (22% crude protein, 5.8% ash, 3,035 kcal/kg; Y. Brown & Sons Feedmill, Hod HaSharon, Israel). Hatchlings and chicks were weighed at DOH, D 1, D 3 and D 7. At DOH, IOF-Gln and IOF-NaCl chick BW increased by 5%, and IOF-Leu chick BW increased by 3%, in comparison to control chicks ($P = 0.040$). At D 1, IOF-Gln and IOF-Leu chick BW was 3% and 4% higher than control chick BW, respectively ($P = 0.042$). At D 7, mean chick BW was 193.75 g and did not differ between groups.

2.2. Tissue sampling

For embryonic intestinal sampling, 6 embryos were randomly selected prior to IOF at E 17, and 6 embryos were randomly selected from each treatment group at E 19 (48 h post IOF procedures). Post–hatch intestinal sampling was conducted on 6 randomly selected chicks from each treatment group at DOH and D 1, D 3 and D 7 (treatment groups and sampling timepoints are depicted in Fig. 1). Embryos were euthanized by cervical dislocation and chicks were euthanized by cervical dislocation, according to established guidelines for animal care and handling by the Hebrew University Institutional Animal Care and Use Committee (IACUC: AG-17-15355-2). The jejunum segment of their small intestines (a 0.5 to 1 cm piece from the midpoint between the duodenal loop and Meckel's diverticulum) was excised, lumen contents were flushed out with phosphate buffered saline (PBS) and tissues were fixed in 3.7% formaldehyde in PBS (pH 7.4) for 24 h at RT. Following fixation, tissues were dehydrated in graded series of ethanol, cleared by Histochoice (Sigma–Aldrich, Rehovot, Israel) and embedded in Paraplast (Sigma–Aldrich, Rehovot, Israel). Tissue blocks were sectioned 5 μm thick with a microtome, and mounted on SuperFrost Plus glass slides (Bar-Naor Ltd., Petah-Tikva, Israel).

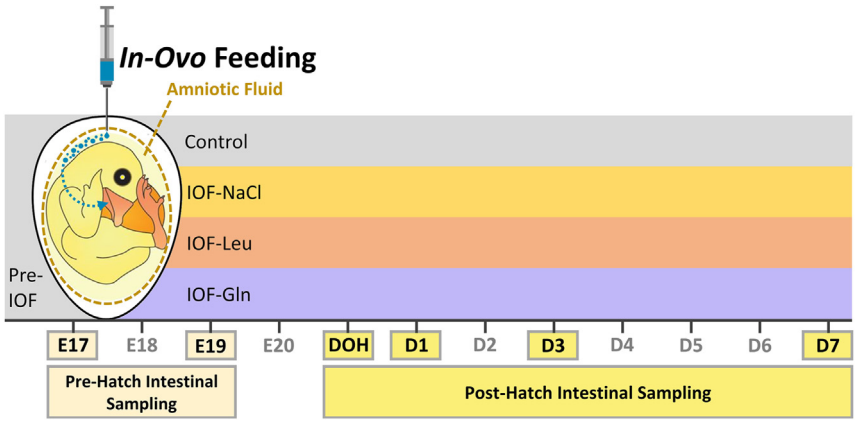

Fig. 1. Description of experimental procedures. In-ovo feeding of glutamine (IOF-Gln, 1% glutamine in 0.4% NaCl), leucine (IOF-Leu, 1% leucine in 0.4% NaCl) and NaCl (IOF–NaCl, 0.75% NaCl) was conducted at embryonic d 17 (E 17). Each nutrient solution was manually injected into the amniotic fluid. Intestinal sampling for downstream procedures was conducted at E 17, prior to IOF treatments, and at E 19, day of hatch (DOH), d 1 post-hatch (D 1), D 3 and D 7 in control (non-injected) and IOF treatment groups.

2.3. Immunofluorescence

Jejunum sections were deparaffinized by Histochoice (Sigma–Aldrich, Rehovot, Israel) and rehydrated in a graded series of ethanol. Antigen retrieval was then performed by heating for 20 min in pH 5.5 citrate buffer (Sigma–Aldrich, Rehovot, Israel). Tissue permeabilization was conducted with 0.1% Tween (Sigma–Aldrich, Rehovot, Israel) in PBS (PBST). Following incubation in a blocking solution of 1% bovine serum albumin (BSA, Sigma–Aldrich, Rehovot, Israel) in PBS, tissues were incubated overnight at 4 C with rabbit anti-Sox9 (1:150, AB5535, Millipore) and mouse anti-PCNA (1:300, sc-56, Santa Cruz) primary antibodies. Tissues were then washed in PBS and PBST, and then incubated for 1 h at RT with donkey anti-Rabbit Alexa Fluor 488 (1:100, 711-545-152, Jackson ImmunoResearch Laboratories, Inc.) and donkey anti-mouse Cy3 (1:100, 715-165-150, Jackson ImmunoResearch Laboratories, Inc.) secondary antibodies. Lastly, tissues were washed in PBS and sealed with fluoromount G with 4′,6-diamidino-2-phenylindole (DAPI) (00-4959, Invitrogen).

2.4. Cell sub-type quantification

Images were acquired by BX40 Olympus microscope (Waltham, MA, USA) at X400 magnifications with a DP73 camera and processed in cellSense Imaging Software (version 1.16). For full-length images of post–hatch villi, images were acquired by EVOS FL Auto Imaging System (Thermo Fisher Scientific) at X200 magnifications and automatically stitched. All images were post-processed for brightness/contrast adjustments and channel merging using ImageJ software. Cellular quantification in embryonic villi was conducted by counting total epithelial cells by DAPI-stained nuclei, and cell sub-types among them were quantified by counting Sox9+ cells and PCNA+/Sox9-cells, in at least 10 villi from 3 replicates in each treatment group, at each timepoint. Post–hatch, DAPI-stained nuclei, Sox9+ cells and PCNA+/Sox9-cells were quantified in at least 10 crypts and 10 villi from 3 replicates in each treatment group, at each timepoint. Cell sub-type percentages were calculated by dividing the number of each cell sub-type by the number of DAPI-stained villus or crypt cells.

2.5. In situ hybridization and mucin staining

Jejunum sections were deparaffinized by Histochoice (Sigma–Aldrich, Rehovot, Israel) and rehydrated in a graded series of ethanol in DEPC-treated water (Sigma–Aldrich, Rehovot, Israel). RNAscope in-situ hybridization (ISH) was performed as described by Wang et al. (2012), according to the manufacturer's protocol (https://acdbio.com). *Lgr5* mRNA transcripts were hybridized using a Gg-Lgr5 probe (XM_425441.4, Cat. No. 480781) and detected using RNAscope 2.5 HD Kit-RED (Cat. No. 322350). *PepT1* mRNA transcripts were hybridized using a Gg-SLC15A1 probe (NM_204365.1, Cat. No. 462341) and detected using RNAscope 2.5 HD Kit-BROWN (Cat. No. 322300). A positive control probe (Gg-PPIB, Cat. No 453371) and a negative control probe DapB (Cat. No. 310043) were used for validation. Tissues were counterstained with 50% hematoxylin (Sigma–Aldrich, Rehovot, Israel) and sealed with DPX mounting medium (Sigma–Aldrich, Rehovot, Israel). For goblet cell quantification, tissues were stained with alcian blue (AB; A5268, Sigma–Aldrich, Rehovot, Israel) for 15 min, rinsed in PBS and sealed with DPX mounting medium (Sigma–Aldrich, Rehovot, Israel).

2.6. Analysis of cell marker localizations and densities

Images were acquired by BX40 Olympus microscope (Waltham, MA, USA) at X100 and X400 magnifications with a DP73 camera and processed with cellSense Imaging Software (version 1.16). For examining the distribution of Lgr5 expression in the embryonic villi at E 19, total villi lengths were measured and divided into equal thirds for determining the bottom, middle and top villi regions. The percentage of Lgr5 punctate expression in each region was calculated by dividing punctate Lgr5 expression counts in each region by total villus punctate Lgr5 expression counts. For examining the extent of PepT1 expression in the embryonic villi at E 19, lengths of the PepT1+ region and the PepT1-region were measured. The percentage of the PepT1+ region within the villus was calculated by dividing the PepT1+ region length by total villus length. For quantifying goblet cells, AB-stained mucins were counted in each villus. Goblet cell densities were calculated by dividing the number of villus goblet cells by villus length.

2.7. Statistical analyses

Data were analyzed using one-way analysis of variance (ANOVA). Differences were considered significant at $P < 0.05$. Post-hoc Tukey–Kramer HSD tests were conducted for detecting significant differences between treatment groups at each timepoint. Significant differences were marked with different uppercase

letters. Graphical data were expressed as means ± standard error means (SEM). All statistical analyses were conducted with JMP Pro 15 software (SAS Institute, Cary, NC, USA).

3. Results

The pre-hatch small intestinal epithelium was visualized at E 17 and E 19 by combined immunofluorescence of proliferation marker PCNA and multipotent cell marker Sox9, along with DAPI nuclear staining. The majority of epithelial cells were PCNA+, and cells at the lower portion of the villus which co-expressed PCNA and Sox9 were regarded as multipotent cells (Fig. 2A and B, arrowheads). PCNA+/Sox9-cells at the upper region of the villus were regarded as progenitor cells (Fig. 2A and B, arrowhead outlines).

Examinations of effects of IOF treatments on the pre-hatch small intestinal epithelium revealed that at E 19, total villus cell counts increased significantly by 19% in IOF-NaCl embryos ($P = 0.005$), 33% in IOF-Leu embryos ($P < 0.001$) and 40% in IOF Gln embryos ($P < 0.001$) in comparison to control embryos (Fig. 2C). Among these cells, Sox9+ multipotent cells were significantly more abundant as a result of IOF treatments: in comparison to control embryos, multipotent cell counts increased by 38% in IOF-NaCl embryos, 50% in IOF-Leu embryos and 52% in IOF-Gln embryos ($P < 0.001$) (Fig. 2C). Furthermore, the percentages of multipotent cells, relative to total villus cell counts, increased from 38% to 44% in all treatment groups (IOF-NaCl: $P = 0.015$; IOF-Leu: $P = 0.018$; IOF-Gln: $P = 0.039$) (Table 1).

IOF-Gln embryos also exhibited a significant, 36% increase in PCNA+/Sox9-progenitor cell counts, compared to control embryos ($P < 0.001$), while the other IOF treatment groups did not differ from control embryos (Fig. 2C). Their percentages, relative to total villus cell counts, were stable between all groups (22% to 27%) (Table 1).

Comparisons of control embryos between E 17 and E 19 revealed that multipotent cell counts and progenitor cell counts significantly increased with age ($P < 0.001$) (Fig. 2C), and the percentages of multipotent cells increased significantly from 29% to 38% ($P < 0.001$) whereas progenitor cell counts remained stable (25% to 27%) (Table 1). These results indicate that by further increasing total cell counts and expanding the Sox9+ multipotent cell niche at E 19, IOF treatments induced early maturation of the small intestinal epithelium.

Post–hatch, the small intestinal epithelium had formed distinct crypts, in which Sox9+ MP cells were located at the bottom region and PCNA+/Sox9-progenitor cells were scattered throughout the crypt epithelium (Fig. 3C and D). The post–hatch villi were devoid of multipotent cells, as all cells were Sox9-negative (results not shown), but contained proliferating (PCNA+) cells at their bottom regions (Fig. 3A and B).

Cell count analyses showed that IOF-Gln significantly increased total villus and crypt cell counts at post–hatch ages, in comparison to control chicks: villi cell counts increased by 26% at DOH ($P = 0.029$), 28% at D 1 ($P < 0.001$) and 12% at D 3 ($P = 0.020$) (Fig. 3E), and crypt cell counts increased by 10% at DOH, D 3 and D 7 ($P = 0.039$, $P = 0.028$, $P = 0.021$, respectively) (Fig. 3F). The sole effect of IOF-Leu and IOF-NaCl on post–hatch epithelial cell counts was a 16% increase in villi cells at D 1, compared to control chicks ($P = 0.005$ and $P = 0.020$, respectively) (Fig. 3E).

However, proliferating (PCNA+) villi cell counts and percentages in all IOF-treatment groups increased in comparison to control chicks at varying post–hatch timepoints. IOF-NaCl chicks exhibited significant increases in proliferating villi cell counts at DOH, D 1, D 3 and D 7 ($P = 0.005$, $P < 0.001$, $P = 0.016$, $P < 0.001$, respectively) (Fig. 3E), with corresponding increases in their percentages, relative to total villi cells, at DOH, D 1 and D 7 ($P = 0.035$, $P = 0.004$, $P = 0.002$, respectively) (Table 2). In IOF-Leu chicks, proliferating villus cell counts and percentages increased at D 1 and D 7 (counts: $P < 0.001$; percentages: $P = 0.001$, $P < 0.001$, respectively) (Fig. 3E) (Table 2). In IOF-Gln chicks, proliferating villus cell counts were significantly higher at DOH, D 1 and D 3 ($P = 0.015$, $P < 0.001$, $P = 0.008$, respectively) (Fig. 3E), while their percentages were significantly higher only at D 1 ($P = 0.012$) (Table 2). These results indicate that the effects of IOF treatments on total villi cell counts did not correspond with the proportions of proliferating villus cells.

Within crypt cells, multipotent cell (Sox9+) counts did not differ significantly between control, IOF-Gln and IOF-Leu chicks (Fig. 3F). However, IOF-Leu chicks exhibited significant, 19% and 17% decreases in multipotent cell counts, compared to control chicks, at DOH and D 1, respectively ($P = 0.024$, $P = 0.006$, respectively) (Fig. 3F). Multipotent cell percentages, relative to total crypt cells, were significantly lower in comparison to control chicks in IOF-Gln at DOH and D 3 ($P = 0.035$, $P = 0.036$, respectively), and in IOF-Leu chicks at DOH and D 1 ($P = 0.003$, $P = 0.001$, respectively) (Table 3), in accordance with the increases in total crypt cell counts. Lastly, progenitor (PCNA+/Sox9-) cell counts and percentages remained stable between treatments at all post–hatch timepoints (Table 3).

To summarize, within the first week post–hatch, IOF-Gln elicited significant expansions of the small intestinal epithelium, as shown at DOH, D 1 and D 3 in the villi and DOH, D 3 and D 7 in the crypts, while IOF-Leu and IOF-NaCl only increased villi cell counts at D 1. The underlying proliferating villus cells and multipotent crypt cells exhibited minor and inconsistent changes in quantities and percentages at these timepoints, while crypt progenitor cell counts and percentages remained stable.

Another indicatory factor of pre-hatch small intestinal maturation is the compartmentalization of ISC and differentiated cell niches during embryonic development. In order to determine whether IOF influenced ISC localizations within the embryonic small intestinal epithelium, we visualized stem cell marker Lgr5 by RNAscope in-situ hybridization (ISH). As the quantity of Lgr5 punctate expression did not differ between treatment groups, we calculated the percentage of Lgr5 punctate expression within the bottom, middle and top regions of the embryonic villus, relative to total villus expression, in each treatment group (Fig. 4). Control embryos at E 17 and E 19 exhibited a similar distribution of Lgr5 expression between regions, while IOF-treated embryos exhibited a significant shift in expression towards the bottom region of the villus, in which percentage of Lgr5 expression significantly increased from 45% in control embryos, to 64% in IOF-NaCl embryos ($P = 0.001$), 71% in IOF-Leu embryos ($P < 0.001$) and 76% in IOF-Gln embryos ($P < 0.001$). Accordingly, the percentage of Lgr5 expression decreased in the middle region from 33% in control embryos to 25% in IOF-NaCl embryos ($P = 0.022$), 24% in IOF-Leu embryos ($P = 0.006$) and 21% in IOF-Gln embryos ($P = 0.002$), and further decreased in the top region from 22% in control embryos to 11% in IOF-NaCl embryos, 5% in IOF-Leu embryos and 3% in IOF-Gln embryos ($P < 0.001$) (Fig. 4C).

These results indicate that all IOF treatments caused a shift in the localization of Lgr5+ stem cells to the bottom region of the villi at E 19, and IOF-Gln elicited the most prominent effect.

Next, RNAscope ISH of absorptive cell marker PepT1 and Alcian Blue staining for goblet cell mucins were conducted in control and IOF-treated embryos in order to determine the effects of IOF on the localization and proportions of differentiated compartment of the embryonic villus. Robust PepT1 expression was evident at the top region and absent from the lower region of the embryonic villus epithelium (Fig. 5A). At E 19, IOF-Gln and IOF-Leu embryos exhibited significant, 1.9-fold and 1.3-fold increases (respectively) in the length of the PepT1-expressing region of the villus (PepT1+), compared to control embryos ($P = 0.001$, $P < 0.001$, respectively),

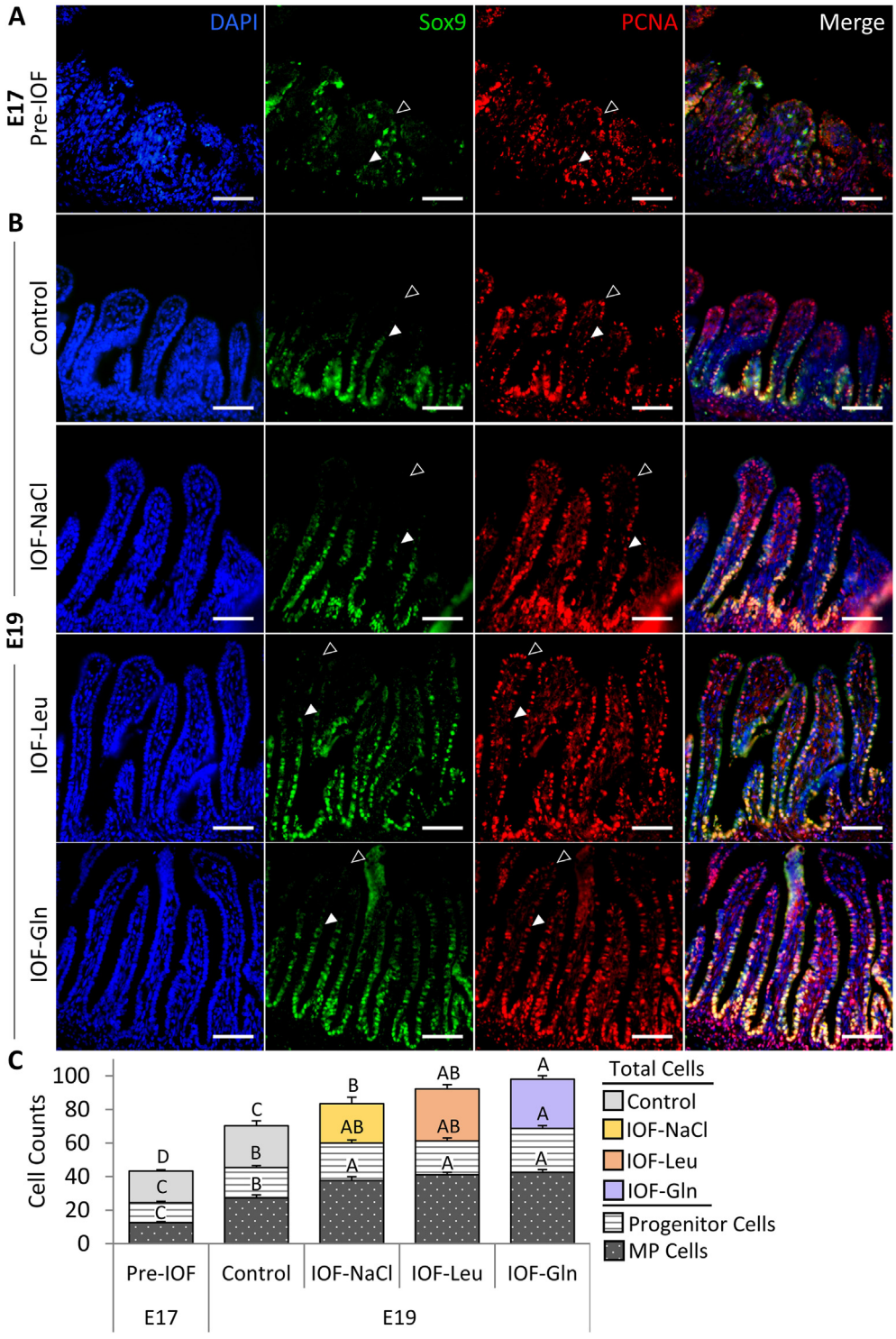

Fig. 2. In-ovo feeding (IOF) increases pre-hatch small intestinal epithelial cell quantities. Immunofluorescence of total epithelial cells by 4′,6-diamidino-2-phenylindole (DAPI) staining (blue), SRY-box transcription factor 9 (Sox9) + cells (green), proliferating cell nuclear antigen (PCNA) + cells (red), and merged images at (A) embryonic d 17 (E 17) (pre-IOF) and at (B) E 19 in control (non-injected), IOF-NaCl, IOF-Leu and IOF-Gln treated embryos. Multipotent Sox9+ cells were located from base to mid portion of each villus and co-localized with PCNA+ cells (arrowheads). Progenitor PCNA+/Sox9- cells were located from the mid to upper portion of each villus (arrowhead outlines). Images were captured at X400 magnifications. Scale bars, 50 μm. (C) Quantification of total epithelial cells, multipotent cells and progenitor cells at E 17 (pre-IOF) and E 19 (post-IOF). Values are means + SEM. Different uppercase letters mark significant differences between age/treatment group for each cell type by Tukey–Kramer HSD, $P < 0.05$.

while the PepT1+ region in IOF-NaCl did not differ from that of control embryos (Fig. 5C). However, the non-PepT1-expressing (PepT1-) region of the villus was significantly longer in IOF-Leu embryos, compared to control embryos ($P < 0.001$), but was unaffected in IOF-Gln embryos (Fig. 5C). Therefore, the percentage of the PepT1+ region length, relative to total villus length, decreased from 86% in the control group, to 65% in the IOF-Leu group ($P < 0.001$), but did not significantly differ between the

Table 1
Multipotent and progenitor cell percentages in the embryonic small intestinal epithelium of control and in-ovo feeding (IOF) -treated embryos (%).[1,2]

Item	Treatment	Multipotent cells	Progenitor cells
E 17	Pre-IOF	28.6 ± 1.8[c]	27.4 ± 2.2
E 19	Control (non-injected)	37.7 ± 1.4[b]	25.4 ± 1.0
	IOF-NaCl	44 ± 1.1[a]	27 ± 1.6
	IOF-Leu	43.9 ± 1.3[a]	21.6 ± 1.7
	IOF-Gln	43.5 ± 1.3[a]	26.7 ± 1.8

E 17 = embryonic d 17; E 19 = embryonic d 19.
[a, b, c] Different letters mark significant differences in each cell sub-type by embryonic age and treatment by Tukey–Kramer HSD, $P < 0.05$. No significant differences were found between values in each treatment group in progenitor cell percentages.
[1] Cell percentage = (100 × Cell sub -Type quantities)/Total cell quantities.
[2] Values are means ± SEM.

IOF-Gln group (91%) and the control group, as well as the Pre-IOF group at E 17 (94%) (Table 4). This indicates that, compared to control embryos, IOF-Gln increased the total amount of PepT1 expression within the embryonic small intestinal epithelium while maintaining a high percentage of PepT1 expression within each villus, while the increases in villi lengths of IOF-Leu embryos decreased the percentages of the PepT1 expressing region.

Goblet cells, stained by Alcian Blue mucin staining (Fig. 5B), did not differ in quantity between treatment groups at E 19 (data not shown). However, their density decreased in the villi of the IOF-Gln group, compared to the control group ($P = 0.027$), while no significant differences were observed between the IOF-NaCl and IOF-Leu groups and the control group (Fig. 5D).

As for the post–hatch small intestinal epithelium, Lgr5 expression was restricted to the crypts and PepT1 expression was robust throughout the entire villus. IOF treatments did not affect localizations and distribution of these cell populations between DOH to D 7. Furthermore, goblet cell counts and densities did not differ between all groups post–hatch (results not shown). Therefore, the effects of IOF on stem (Lgr5+) and differentiated (PepT1+ and goblet) cell populations were evident only in the embryonic villus, 48 h post nutrient administration.

4. Discussion

This study has shown that pre-hatch administration of glutamine and leucine by IOF during a critical timepoint in small intestinal development enhanced peri-hatch small intestinal maturation by expanding and compartmentalizing multipotent, proliferating and differentiated epithelial cell populations.

Characterization of multipotency and proliferation the pre-hatch small intestinal epithelium by PCNA and Sox9 immunofluorescence revealed that among epithelial PCNA+ proliferating cells, Sox9+ cells were located at the bottom half of the villi and Sox9- cells were located at the upper half of the villi. This epithelial structuring was comparable to that of the adult crypt in mammals, in which the basal region is mainly comprised of multipotent stem cells, and in the upper region, proliferating cells lose their stemness and transiently amplify towards a definitive, differentiated state (Carulli et al., 2014). We therefore characterized Sox9+ cells as MP cells and PCNA+/Sox9- cells as progenitor cells.

IOF of glutamine (IOF-Gln) significantly affected the dynamics of small intestinal epithelial maturation at E 19, 48 h post-administration, as the quantities of total epithelial cells and the underlying multipotent and progenitor cells increased, along with an increase in the percentage of multipotent cells, relative to total epithelial cells, compared to control embryos. These results indicate that glutamine availability in the intestinal lumen, following amniotic ingestion by IOF-Gln embryos, resulted in increased proliferation of multipotent cells. This is in accordance with findings from previous studies, that showed direct stimulation of crypt cell proliferation by glutamine, following its uptake by small intestinal epithelial cells (Rhoads and Wu, 2009). In addition to the higher quantities and percentages of multipotent cells, which indicate an increased potential to generate functional differentiated cells, the increased quantities of progenitor cells in IOF-Gln embryos indicate that a higher number of cells advanced beyond the niche towards a mature, differentiated state.

For further comprehension of the effects of IOF-Gln on the developing multipotent cell niche, we investigated the effects of IOF-Gln on the expression of stem cell marker Lgr5. Though previous studies of glutamine supplementation resulted in inconsistent or non-prominent effects on expression levels of Lgr5 (Chen et al., 2019), we were able to identity significant changes in the localizations of Lgr5 mRNA expression through RNAscope ISH, a method that has been previously proven useful for high specificity ISC identification in chicken (Zhang and Wong, 2018). We found that IOF-Gln significantly shifted Lgr5 expression towards the bottom region of the villus at E 19, compared to control embryos, thus promoting the zonation of stem cells into dedicated regions. An elegant study by Shyer et al. (2015) demonstrated that stem cell localizations shift towards the villus bottom during the final stages of chick embryonic development, as a result of morphometric expansions of the villi. Our results showed a similar pattern in the small intestinal epithelium of IOF-Gln embryos at E 19, in which Lgr5 expression was highly concentrated at the bottom regions and almost absent from villi tips, in comparison to the more uniform distribution of Lgr5 expression along the shorter villi of control embryos. We hypothesize that the induced expansion of the villus epithelium in IOF-Gln embryos, compared to control embryos, promoted stem cell zonation at villi bottoms through enhanced BMP signaling along the upper regions of the villi, which locally inhibits stem cell self-renewal by suppressing Wnt signaling (He et al., 2004; Shyer et al., 2015).

Visualization of differentiated cells by PepT1, a marker for absorptive intestinal cells (Fei et al., 2000), revealed robust expression at the top region of the embryonic villus epithelium, and expression ceased at the lower regions. This finding was in accordance with previous findings in chick embryos (Zhang and Wong, 2017) and comparable to PepT1 expression in small intestinal villi tips in mice (Moor et al., 2018). In IOF-Gln chicks, the PepT1 expressing region of the villus was significantly longer than in control chicks, indicating increased differentiation into mature, absorptive cells.

This result may be explained by induction of BMP signaling through villus elongation, which promoted differentiation over stem cell self-renewal along the villus (He et al., 2004; Shyer et al., 2015). Furthermore, BMP suppression of stem cell self-renewal involves suppression of Akt activity (He et al., 2004). Similarly, glutamine supplementation was also found to decrease the levels of activated Akt (Larson et al., 2007; Ren et al., 2014). Therefore, it is possible that IOF-Gln enhanced the differentiation of villi cells by inhibiting stem cell self-renewal along the villus through BMP and Akt-mediated signaling.

In contrast, IOF-Gln did not alter the number of goblet cells in the embryonic villus. Since the villi of IOF-Gln embryos were composed of a significantly higher number of cells, goblet cell densities in IOF-Gln embryos were significantly lower than in control embryos. Similar to our findings, glutamine supplementation in weaning mice did not affect goblet cell counts (Chen et al., 2018), and goblet cell formation in murine enteroids was independent of glutamine (Moore et al., 2015). We therefore conclude that IOF-Gln specifically promoted differentiation of the absorptive cell lineage over the secretory cell lineage, possibly through Notch-mediated signaling (Stanger et al., 2005). By hatch, goblet cell

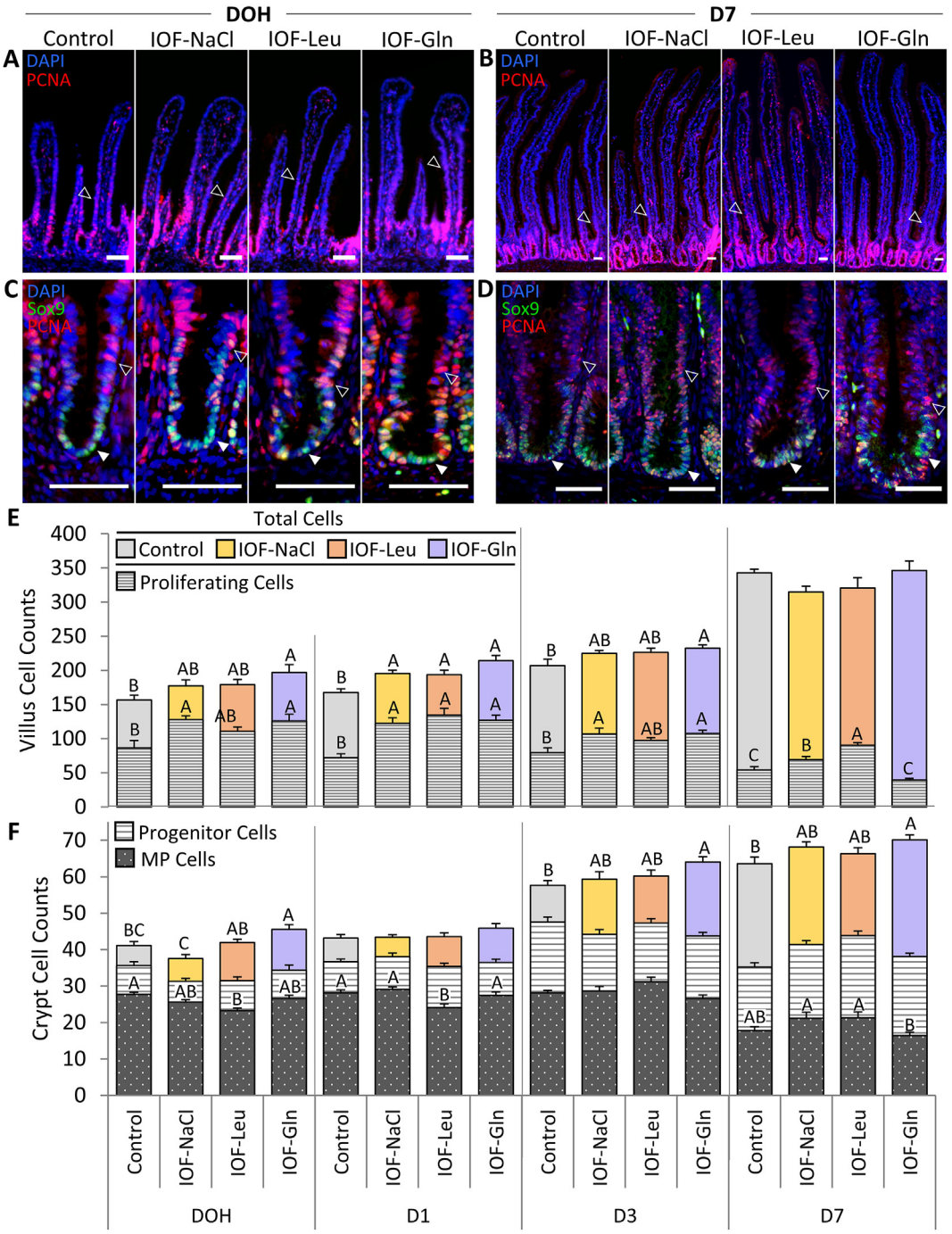

Fig. 3. In-ovo feeding (IOF) increases post–hatch small intestinal epithelial cell quantities. (A, B) Immunofluorescence of total villus epithelial cells by DAPI staining (blue), merged with proliferating cell nuclear antigen (PCNA)+ staining (red) at day of hatch (DOH) (A) and d 7 post-hatch (D 7) (B) in control (non-injected), IOF-NaCl, IOF-Leu and IOF-Gln treated chicks. Images were captured at X200 magnifications and automatically stitched. Arrowhead outlines indicate PCNA+ proliferating cells at the bottom regions of the villi. (C, D) Immunofluorescence of total crypt epithelial cells by DAPI staining (blue), merged with PCNA staining (Red) and SRY-box transcription factor 9 (Sox9) staining at DOH (C) and D 7 (D) in control, IOF-NaCl, IOF-Leu and IOF-Gln treated chicks. Images were captured at X400 magnifications. Multipotent Sox9+ cells were located at the base of each crypt and co-localized with PCNA+ cells (C, D, arrowheads). PCNA+/Sox9- progenitor cells were scattered throughout the crypt epithelium (C, D, arrowhead outlines). Scale bars, 50 μm. (E) Quantification of total villus cells and villus proliferating cells from DOH to D 7 in control (non-injected) and IOF-treated chicks. (F) Quantification of total crypt cells, Sox9+ multipotent cells and PCNA+/Sox9- progenitor cells from DOH to D 7 in control (non-injected) and IOF-treated chicks. Values are means ± SEM. Different uppercase letters mark significant differences between age/treatment group for each cell type by Tukey–Kramer HSD, $P < 0.05$.

densities in IOF-Gln chicks did not differ from those of control chicks, therefore mucin secretion potential was not compromised as a result of IOF-Gln.

IOF of leucine (IOF-Leu) also resulted in enhanced small intestinal maturation at E 19 through increased cellular proliferation and differentiation, compared to control embryos, but to a lesser extent than IOF-Gln. IOF-Leu increased total epithelial cell counts and Sox9+ multipotent cell counts and percentages, relative to total cell counts, in comparison to control embryos. However, villus cell quantities were lower than in IOF-Gln embryos. Moreover, PCNA+/

Table 2
Post–hatch villus proliferating cell percentages in control and in-ovo feeding (IOF) -treated chicks (%).[1,2]

Item	Control(non-injected)	IOF-NaCl	IOF-Leu	IOF-Gln
DOH	55.9 ± 6.6^{b}	72.5 ± 2.4^{a}	62.9 ± 3.4^{ab}	65.4 ± 4.5^{ab}
D 1	44.3 ± 6.6^{b}	62.4 ± 3.7^{a}	68.7 ± 4.4^{a}	61.3 ± 3.9^{a}
D 3	39.4 ± 2.9^{a}	47.9 ± 3.8^{a}	43.4 ± 1.5^{a}	46.5 ± 2.0^{a}
D 7	15.7 ± 1.3^{c}	22.3 ± 1.5^{b}	29.6 ± 1.7^{a}	11.5 ± 0.6^{c}

DOH = d of hatch; D 1 = d 1 post-hatch: D 3 = d 3 post-hatch; D 7 = d 7 post-hatch.
[a, b, c] Different letters mark significant differences between treatment groups at each day by Tukey–Kramer HSD, $P < 0.05$. No significant differences were found between values in each treatment group at each day in proliferating cell percentages.
[1] Cell percentage = 100 × Proliferating cell quantities/Total villus cell quantities.
[2] Values are means ± SEM.

Sox9- progenitor cell quantities in IOF-Leu embryos did not differ from control embryos, in contrast to IOF-Gln embryos. This result indicates that despite the increased proportions of multipotent cell niche, the quantities of cells that transitioned from multipotency towards differentiation did not differ from those in control embryos, indicating a limited effect of IOF-Leu on small intestinal epithelial maturation at E 19. Indeed, post–hatch effects of IOF-Leu were limited, as villi cell counts did not differ from those of control chicks, except at D 1. However, at D 7, villi proliferating cell counts were significantly higher in IOF-Leu chicks, compared to all other groups. This may be due to a delayed effect of leucine on cell proliferation. Since D 7 was the last day of sampling, our data does not provide evidence for this hypothesis.

A possible explanation for the differences between the effects of IOF-Leu and IOF-Gln can be derived from the fact that dietary leucine acts as a nitrogen donor for glutamine synthesis (Nie et al., 2018). Therefore, IOF-Leu may have promoted the molecular pathway of glutamine-induced cellular proliferation in the small intestinal epithelium in an indirect manner, resulting in decreased efficiency, compared to IOF-Gln. Another possible explanation is that the maximal effect of leucine supplementation on small

Table 3
Multipotent and progenitor cell percentages in the crypt epithelium of control and in-ovo feeding (IOF) -treated chicks (%).[1,2]

Item	Multipotent cells				Progenitor cells			
	Control (non-injected)	IOF-NaCl	IOF-Leu	IOF-Gln	Control (non-injected)	IOF-NaCl	IOF-Leu	IOF-Gln
DOH	67.5 ± 2.1^{a}	69 ± 1.8^{a}	56 ± 2.4^{b}	58.3 ± 2.7^{b}	19.6 ± 1.6	14.6 ± 1.4	19.6 ± 1.7	16.4 ± 1.6
D 1	65.8 ± 1.8^{a}	66.8 ± 1.8^{a}	55.9 ± 1.8^{b}	60.3 ± 1.6^{ab}	19.7 ± 1.8	20.9 ± 1.6	25.6 ± 1.9	19.7 ± 1.4
D 3	49.5 ± 2.5^{a}	48.5 ± 1.9^{a}	52.5 ± 1.9^{ab}	41.9 ± 1.5^{b}	31.6 ± 1.8	26.2 ± 1.8	26.9 ± 1.5	26.6 ± 1.5
D 7	28 ± 1.5^{ab}	31 ± 1.5^{a}	31.8 ± 1.5^{a}	23.8 ± 1.4^{b}	27.4 ± 1.7	29.8 ± 2.3	33.5 ± 1.9	31.2 ± 1.3

DOH = d of hatch; D 1 = d 1 post-hatch: D 3 = d 3 post-hatch; D 7 = d 7 post-hatch.
[a, b] Different uppercase letters mark significant differences between treatment groups at each day by Tukey–Kramer HSD, $P < 0.05$. No significant differences were found between means in each treatment group at each day in proliferating cell percentages.
[1] Cell percentage = 100 × (Cell sub -Type quantities)/Total cell quantities.
[2] Values are means ± SEM.

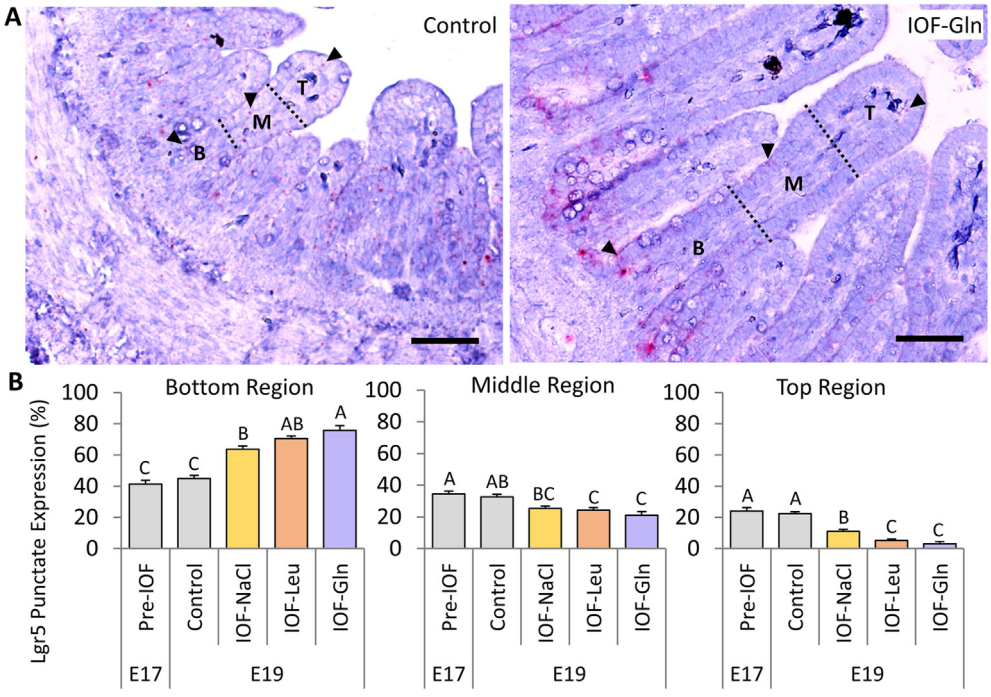

Fig. 4. In-ovo feeding (IOF) shifts pre-hatch stem cell localizations toward villus bottoms. (A, B) Representative images of RNAscope in-situ hybridization (ISH) of stem cell marker leucine-rich repeat containing G-protein coupled receptor 5 (Lgr5) at embryonic day 19 (E 19) in the bottom (B), middle (M) and top (T) regions of each villus (separated by dotted lines) in control (non-injected) (A) and IOF-Gln embryos (B). Arrowheads indicate Lgr5 punctate expression within each region. Lgr5 probes were visualized with fast-red and tissues were counterstained with hematoxylin. Images were captured at X200 magnifications. Scale bars, 50 μm. (C) Percentage of Lgr5 punctate expression in each villus region, relative to total Lgr5 expression in the entire villus. Values are means ± SEM. Different uppercase letters mark significant differences between age/treatment group in each villus region by Tukey–Kramer HSD, $P < 0.05$.

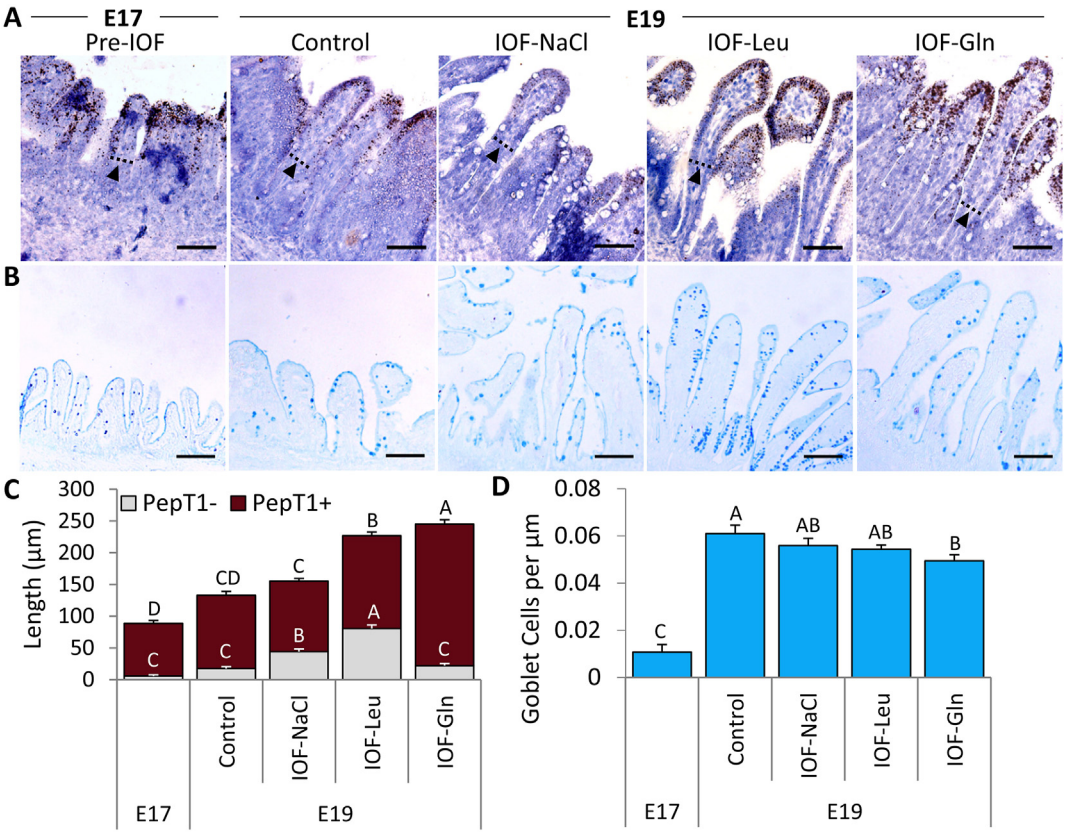

Fig. 5. In-ovo feeding (IOF) lengthens pre-hatch absorptive cell marker expressing regions. (A) RNAscope in-situ hybridization (ISH) of absorptive cell marker peptide transporter 1 (PepT1) at embryonic d 17 (E 17) (pre-IOF) and E 19 in control (non-injected), IOF-NaCl, IOF-Leu and IOF-Gln treated embryos. PepT1 probes were visualized with 3,3′-diaminobenzidine (DAB) and tissues were counterstained with hematoxylin. Dotted lines and arrowheads mark the limit between the PepT1 expressing-region and non PepT1 expressing-region within the villus. (B) Goblet cells were visualized by Alcian Blue acidic mucin staining at E 17 (pre-IOF) and E 19 in control (non-injected), IOF-NaCl, IOF-Leu and IOF-Gln treated embryos. Images were captured at X400 magnifications. Scale bars, 50 μm. (C) Length of non-PepT1 expressing (PepT1-, grey) and PepT1-expressing (PepT1+, brown) segments within each villus at E 17 (pre-IOF) and E 19 in control (non-injected) and IOF-treated embryos. (D) Goblet cell densities at E 17 (pre-IOF) and E 19 in control (non-injected) and IOF-treated embryos. Values are means ± SEM. Different uppercase letters mark significant differences between age/treatment group by Tukey–Kramer HSD, $P < 0.05$.

Table 4
Percentages of PepT1-expressing region lengths, relative to total villi lengths of control and in-ovo feeding (IOF) -treated chicks (%).[1,2]

Item	Treatment	PepT1+ region
E 17	Pre-IOF	94.4 ± 1.7[a]
E 19	Control (non-injected)	85.8 ± 2.4[a]
	IOF-NaCl	72.5 ± 1.9[b]
	IOF-Leu	64.8 ± 2.3[b]
	IOF-Gln	90.6 ± 1.5[a]

PepT1 = peptide transporter 1; E 17 = embryonic d 17; E 19 = embryonic d 19.
[a, b] Different uppercase letters mark significant differences by Tukey–Kramer HSD, $P < 0.05$.
[1] Percentage of region length = 100 × [PepT1+Segment length (μm)/Total villus length (μm)].
[2] Values are means ± SEM.

intestinal proliferation may require an addition of other branched-chain amino acids (BCAA). We base this hypothesis on previous findings in pigs, which showed that leucine supplementation was most effective in enhancing epithelial cell proliferation when combined with isoleucine and valine (Duan et al., 2018). Furthermore, amino acid profiling of the amniotic fluid of E 17 chick embryos revealed that leucine content was higher than isoleucine and valine (Omede et al., 2017). These data indicate that amniotic administration of an additional 6 mg of leucine by IOF may have disrupted BCAA ratios, resulting in a reduced induction of small intestinal epithelial proliferation, compared to the potential effects of IOF of leucine combined with other BCAA.

However, IOF-Leu promoted stem cell zonation in a manner similar to IOF-Gln, as was visualized by Lgr5 expression. This result may also be attributed to the significant expansions of the villus epithelium in IOF-Leu chicks, compared to control chicks, which may have shifted stem cell localizations towards the bottom of the villus through BMP signaling (Shyer et al., 2015).

Examinations of differentiation at E 19 by PepT1 expression, revealed that the proportions of the differentiated region of the villi were significantly smaller in IOF-Leu embryos, compared to IOF-Gln embryos. The PepT1+ region was shorter and the percentage of its length, relative to total villus length, was reduced, compared to IOF-Gln embryos. IOF-Leu therefore resulted in a slower rate of differentiation, compared to IOF-Gln embryos, and a reduced absorptive potential within their small intestine at E 19. Additionally, goblet cell densities in IOF-Leu embryos did not differ from control embryos, indicating that IOF-Leu did not affect the rate of goblet cell differentiation.

It should be noted that IOF of NaCl, the diluent for glutamine and leucine in the IOF solutions, also enhanced small intestinal development at E 19, 48 h post-administration, through increased total epithelial cell counts, multipotent cell counts and percentages, relative to total villus cell counts, and zonation of Lgr5 mRNA at villus bottoms. However, proliferating cell counts and the extent of differentiation in IOF-NaCl embryos did not differ from control

embryos. The beneficial effects of IOF-NaCl on small intestinal epithelial maturation may be attributed to enhanced activity of nutrient transporters, mediated by increased levels of Na^+ and Cl^- ions in the intestinal lumen, following the ingestion of the NaCl-enriched amniotic fluid. A variety of nutrient transporters, including Na–K^+-ATPase and transporters for peptides, amino acids, sugars, vitamins and minerals, depend on Na^+ and Cl^- ion exchange (Kiela and Ghishan, 2016). Therefore, we hypothesize that IOF-NaCl induced small intestinal epithelial proliferation through enhanced absorption of amniotic fluid nutrients.

Taken together, IOF elicited significant effects on small intestinal development at E 19, 48 h post administration, in a nutrient-specific manner. While IOF of glutamine, leucine and NaCl promoted epithelial expansion and increased proliferation and zonation of the multipotent cell niche, only IOF of glutamine promoted cellular proliferation to the extent that significantly increased the progenitor cell population and promoted differentiation into absorptive cells.

These advancements in small intestinal development at the final stage of embryonic development in IOF-Gln embryos further impacted the small intestinal epithelium during the first week post–hatch, in which total villus cell counts were significantly higher at DOH, D 1 and D 3, and total crypt cell counts were significantly higher at DOH, D 3 and D 7, compared to control chicks. In contrast, IOF of leucine and NaCl only increased villi cell counts at D 1. Increased villus cell counts at D 1 were previously found to be a result of primary feeding (Reicher et al., 2020), therefore the combination of IOF and primary exogenous feeding may have elicited a prominent effect within the first 24 h post–hatch. Furthermore, general decreases in the percentages of crypt multipotent cells and villus proliferating cells were observed during the first week post–hatch, in accordance with previous studies (Uni et al., 2000; Reicher et al., 2020), and were inconsistently affected by IOF, indicating that the effects of IOF on cellular proliferation and differentiation are most prominent pre-hatch.

Nevertheless, since the post–hatch small intestinal epithelium in all groups portrayed similar stem, proliferating and differentiated cell localizations, in accordance with previous studies (Reicher et al., 2020; Uni et al., 1998, 2003a; Zhang and Wong, 2017, 2018), the expanded post–hatch villus epithelium in IOF-Gln chicks was made up of a larger PepT1-expressing surface area, indicating greater absorptive capacity, compared to control chicks.

Improved nutrient utilization during the critical period of transition from egg-based nutrition to exogenous feed can alleviate the nutritional and energetic limitations that broiler chicks face during this period (Moran, 2007). IOF is therefore a highly applicative method for supporting small intestinal development during the critical peri-hatch period, in order to improve small intestinal functionality and nutrient utilization. Furthermore, IOF provides an important tool for examining a variety of effects of specific nutrients and metabolites on small intestinal development, functionality, immunity and microbial interactions (Hou and Tako, 2018; Roto et al., 2016). This study is the first to uncover a cellular basis for the stimulatory effects of IOF on small intestinal maturation, thus shedding light on the link between primary nutritional stimulation and small intestinal development.

Author contributions

Naama Reicher: conceptualization, formal analysis, investigation, methodology, visualization, writing - original draft. **Tal Melkman-Zehavi**: investigation, methodology, project administration, supervision. **Jonathan Dayan:** investigation. **Eric A. Wong:** funding acquisition, resources, supervision, writing - review & editing. **Zehava Uni:** conceptualization, funding acquisition, methodology, project administration, resources, supervision, writing - review & editing.

Declaration of competing interest

We declare that we have no financial and personal relationships with other people or organizations that can inappropriately influence our work, and there is no professional or other personal interest of any nature or kind in any product, service and/or company that could be construed as influencing the content of this paper.

Acknowledgements

This research was supported by Research Grant No. US-5074-18CR from the United States - Israel Binational Agricultural Research and Development (BARD) Fund.

References

Barker N, van Es JH, Kuipers J, Kujala P, van den Born M, Cozijnsen M, et al. Identification of stem cells in small intestine and colon by marker gene Lgr5. Nature 2007;449(7165):1003–7. https://doi.org/10.1038/nature06196.

Bartell SM, Batal AB. The effect of supplemental glutamine on growth performance, development of the gastrointestinal tract, and humoral immune response of broilers. Poultry Sci 2007;86(9):1940–7. https://doi.org/10.1093/ps/86.9.1940.

Blache P, van de Wetering M, Duluc I, Domon C, Berta P, Freund JN, et al. SOX9 is an intestine crypt transcription factor, is regulated by the Wnt pathway, and represses the CDX2 and MUC2 genes. J Cell Biol 2004;166(1):37–47. https://doi.org/10.1083/jcb.200311021.

Carulli AJ, Samuelson LC, Schnell S. Unraveling intestinal stem cell behavior with models of crypt dynamics. Integr Biol (Camb). 2014;6(3):243–57. https://doi.org/10.1039/c3ib40163d.

Chang Y, Cai H, Liu G, Chang W, Zheng A, Zhang S, et al. Effects of dietary leucine supplementation on the gene expression of mammalian target of rapamycin signaling pathway and intestinal development of broilers. Anim Nutr 2015;1(4):313–9. https://doi.org/10.1016/j.aninu.2015.11.005.

Cheled-Shoval SL, Amit-Romach E, Barbakov M, Uni Z. The effect of in ovo administration of mannan oligosaccharide on small intestine development during the pre- and posthatch periods in chickens. Poultry Sci 2011;90(10):2301–10. https://doi.org/10.3382/ps.2011-01488.

Chen S, Xia Y, Zhu G, Yan J, Tan C, Deng B, et al. Glutamine supplementation improves intestinal cell proliferation and stem cell differentiation in weanling mice. Food Nutr Res 2018;62. https://doi.org/10.29219/fnr.v62.1439.

Chen Y, Tsai YH, Tseng BJ, Tseng SH. Influence of growth hormone and glutamine on intestinal stem cells: a narrative review. Nutrients 2019;11(8):1941. https://doi.org/10.3390/nu11081941.

Coëffier M, Claeyssens S, Bensifi M, Lecleire S, Boukhettala N, Maurer B, et al. Influence of leucine on protein metabolism, phosphokinase expression, and cell proliferation in human duodenum. Am J Clin Nutr 2011;93(6):1255–62. https://doi.org/10.3945/ajcn.111.013649.

Dai D, Wu SG, Zhang HJ, Qi GH, Wang J. Dynamic alterations in early intestinal development, microbiota and metabolome induced by in ovo feeding of L-arginine in a layer chick model. J Anim Sci Biotechnol 2020;11:19. https://doi.org/10.1186/s40104-020-0427-5.

Domeneghini C, Di Giancamillo A, Bosi G, Arrighi S. Can nutraceuticals affect the structure of intestinal mucosa? Qualitative and quantitative microanatomy in L-glutamine diet-supplemented weaning piglets. Vet Res Commun 2006;30(3):331–42. https://doi.org/10.1007/s11259-006-3236-1.

Duan Y, Tan B, Li J, Liao P, Huang B, Li F, et al. Optimal branched-chain amino acid ratio improves cell proliferation and protein metabolism of porcine enterocytesin vivo and in vitro. Nutrition 2018;54:173–81. https://doi.org/10.1016/j.nut.2018.03.057.

Fei YK, Sugawara M, Liu JC, Li HW, Ganapathy V, Ganapathy ME, et al. cDNA structure, genomic organization, and promoter analysis of the mouse intestinal peptide transporter PEPT1. Biochim Biophys Acta 2000;1492:145–54. https://doi.org/10.1016/s0167-4781(00)00101-9.

Foye OT, Ferket PR, Uni Z. The effects of in ovo feeding arginine, beta-hydroxy-beta-methyl-butyrate, and protein on jejunal digestive and absorptive activity in embryonic and neonatal Turkey poults. Poultry Sci 2007;86(11):2343–9. https://doi.org/10.3382/ps.2007-00110.

Gao T, Zhao M, Zhang L, Li J, Yu L, Lv P, et al. Effect of in ovo feeding of l-arginine on the hatchability, growth performance, gastrointestinal hormones, and jejunal digestive and absorptive capacity of posthatch broilers. J Anim Sci 2017;95(7):3079–92. https://doi.org/10.2527/jas.2016.0465.

Geyra A, Uni Z, Sklan D. Enterocyte dynamics and mucosal development in the posthatch chick. Poultry Sci 2001a;80(6):776–82. https://doi.org/10.1093/ps/80.6.776.

Geyra A, Uni Z, Sklan D. The effect of fasting at different ages on growth and tissue dynamics in the small intestine of the young chick. Br J Nutr 2001b;86(1):53–61. https://doi.org/10.1079/bjn2001368.
Hamilton HL. Lillie's development of the chick. An Introduction to Embryology. In: Revised by Hamilton, HL. New York, NY: H. Holt and Co.; 1952.
Haramis AP, Begthel H, van den Born M, van Es J, Jonkheer S, Offerhaus GJ, et al. De novo crypt formation and juvenile polyposis on BMP inhibition in mouse intestine. Science 2004;303(5664):1684–6. https://doi.org/10.1126/science.1093587.
He XC, Zhang J, Tong WG, Tawfik O, Ross J, Scoville DH, Tian Q, Zeng X, He X, Wiedemann LM, Mishina Y, Li L. BMP signaling inhibits intestinal stem cell self-renewal through suppression of Wnt-beta-catenin signaling. Nat Genet 2004;36(10):1117–21. https://doi.org/10.1038/ng1430.
Hou T, Tako E. The in ovo feeding administration (gallus gallus)-an emerging in vivo approach to assess bioactive compounds with potential nutritional benefits. Nutrients 2018;10(4):418. https://doi.org/10.3390/nu10040418.
Kadam MM, Barekatain MR, Bhanja SK, Iji PA. Prospects of in ovo feeding and nutrient supplementation for poultry: the science and commercial applications–a review. J Sci Food Agric 2013;93(15):3654–61. https://doi.org/10.1002/jsfa.6301.
Kiela PR, Ghishan FK. Physiology of intestinal absorption and secretion. Best Pract Res Clin Gastroenterol 2016;30(2):145–59. https://doi.org/10.1016/j.bpg.2016.02.007.
Kubben FJ, Peeters-Haesevoets A, Engels LG, Baeten CG, Schutte B, Arends JW, et al. Proliferating cell nuclear antigen (PCNA): a new marker to study human colonic cell proliferation. Gut 1994;35(4):530–5. https://doi.org/10.1136/gut.35.4.530.
Larson SD, Li J, Chung DH, Evers BM. Molecular mechanisms contributing to glutamine-mediated intestinal cell survival. Am J Physiol Gastrointest Liver Physiol 2007 Dec;293(6):G1262–71. https://doi.org/10.1152/ajpgi.00254.2007. Epub 2007 Oct 4. PMID: 17916648; PMCID: PMC2432018.
Moor AE, Harnik Y, Ben-Moshe S, Massasa EE, Rozenberg M, Eilam R, Bahar Halpern K, Itzkovitz S. Spatial reconstruction of single enterocytes uncovers broad zonation along the intestinal villus axis. Cell 2018;175(4):1156–67. https://doi.org/10.1016/j.cell.2018.08.063. e15.
Moore SR, Guedes MM, Costa TB, Vallance J, Maier EA, Betz KJ, Aihara E, Mahe MM, Lima AA, Oriá RB, Shroyer NF. Glutamine and alanyl-glutamine promote crypt expansion and mTOR signaling in murine enteroids. Am J Physiol Gastrointest Liver Physiol 2015;308(10):G831–9. https://doi.org/10.1152/ajpgi.00422.2014.
Moran Jr ET. Nutrition of the developing embryo and hatchling. Poultry Sci 2007;86(5):1043–9. https://doi.org/10.1093/ps/86.5.1043.
Nie C, He T, Zhang W, Zhang G, Ma X. Branched chain amino acids: beyond nutrition metabolism. Int J Mol Sci 2018 Mar 23;19(4):954. https://doi.org/10.3390/ijms19040954. PMID: 29570613; PMCID: PMC5979320.
Omede AA, Bhuiyan MM, Lslam AF, Iji PA. Physico-chemical properties of late-incubation egg amniotic fluid and a potential in ovo feed supplement. Asian-Australas J Anim Sci 2017;30(8):1124–34. https://doi.org/10.5713/ajas.16.0677.
Potten CS, Loeffler M. Stem cells: attributes, cycles, spirals, pitfalls and uncertainties. Lessons for and from the crypt. Development 1990;110(4):1001–20.
Reicher N, Melkman-Zehavi T, Dayan J, Uni Z. It's all about timing: early feeding promotes intestinal maturation by shifting the ratios of specialized epithelial cells in chicks. Front Physiol 2020;11:596457. https://doi.org/10.3389/fphys.2020.596457.
Ren W, Yin J, Wu M, Liu G, Yang G, Xion Y, et al. Serum amino acids profile and the beneficial effects of L-arginine or L-glutamine supplementation in dextran sulfate sodium colitis. PLoS One 2014;9(2):e88335. https://doi.org/10.1371/journal.pone.0088335.
Rhoads JM, Argenzio RA, Chen W, Rippe RA, Westwick JK, Cox AD, Berschneider HM, et al. L-glutamine stimulates intestinal cell proliferation and activates mitogen-activated protein kinases. Am J Physiol 1997;272(5 Pt 1):G943–53. https://doi.org/10.1152/ajpgi.1997.272.5.G943.
Rhoads JM, Wu G. Glutamine, arginine, and leucine signaling in the intestine. Amino Acids 2009;37(1):111–22. https://doi.org/10.1007/s00726-008-0225-4.
Romanoff AL. The avian embryo: structural and functional development. New York, NY: Macmillan; 1960.
Roto SM, Kwon YM, Ricke SC. Applications of in ovo technique for the optimal development of the gastrointestinal tract and the potential influence on the establishment of its microbiome in poultry. Front Vet Sci 2016;17(3):63. https://doi.org/10.3389/fvets.2016.00063.
Shyer AE, Huycke TR, Lee C, Mahadevan L, Tabin CJ. Bending gradients: how the intestinal stem cell gets its home. Cell 2015;161(3):569–80. https://doi.org/10.1016/j.cell.2015.03.041.
Shyer AE, Tallinen T, Nerurkar NL, Wei Z, Gil ES, Kaplan DL, et al. Villification: how the gut gets its villi. Science 2013;342(6155):212–8. https://doi.org/10.1126/science.1238842.
Stanger BZ, Datar R, Murtaugh LC, Melton DA. Direct regulation of intestinal fate by Notch. Proc Natl Acad Sci U S A 2005;102(35):12443–8. https://doi.org/10.1073/pnas.0505690102.
Sun Y, Wu Z, Li W, Zhang C, Sun K, Ji Y, et al. Dietary L-leucine supplementation enhances intestinal development in suckling piglets. Amino Acids 2015;47(8):1517–25. https://doi.org/10.1007/s00726-015-1985-2.
Tako E, Ferket PR, Uni Z. Effects of in ovo feeding of carbohydrates and beta-hydroxy-beta-methylbutyrate on the development of chicken intestine. Poultry Sci 2004;83(13):2023–8. https://doi.org/10.1093/ps/83.12.2023.
Uni Z, Platin R, Sklan D. Cell proliferation in chicken intestinal epithelium occurs both in the crypt and along the villus. J Comp Physiol B 1998;168(4):241–7. https://doi.org/10.1007/s003600050142.
Uni Z, Geyra A, Ben-Hur H, Sklan D. Small intestinal development in the young chick: crypt formation and enterocyte proliferation and migration. Br Poultry Sci 2000;41(5):544–51. https://doi.org/10.1080/00071660020009054.
Uni Z, Ferket PR. Enhancement of development of oviparous species by in ovo feeding. Raleigh, NC: North Carolina State Univ; 2003. Yissum Research Development Company of the Hebrew Univ of Jerusalem, Jerusalem, IL, assignees. US Pat. No. 6,592,878. Washington, DC: US Patent and Trademark Office.
Uni Z, Smirnov A, Sklan D. Pre- and posthatch development of goblet cells in the broiler small intestine: effect of delayed access to feed. Poultry Sci 2003a;82(2):320–7. https://doi.org/10.1093/ps/82.2.320.
Uni Z, Tako E, Gal-Garber O, Sklan D. Morphological, molecular, and functional changes in the chicken small intestine of the late-term embryo. Poultry Sci 2003b;82(11):1747–54. https://doi.org/10.1093/ps/82.11.1747.
Wang F, Flanagan J, Su N, Wang LC, Bui S, Nielson A, et al. RNAscope: a novel in situ RNA analysis platform for formalin-fixed, paraffin-embedded tissues. J Mol Diagn 2012;14(1):22–9. https://doi.org/10.1016/j.jmoldx.2011.08.002.
Wang J, Lin J, Wang J, Wu S, Qi G, Zhang H, et al. Effects of in ovo feeding of N-acetyl-L-glutamate on early intestinal development and growth performance in broiler chickens. Poultry Sci 2020;99(7):3583–93. https://doi.org/10.1016/j.psj.2020.04.003.
Yair R, Shahar R, Uni Z. In ovo feeding with minerals and vitamin D3 improves bone properties in hatchlings and mature broilers. Poultry Sci 2015;94(11):2695–707. https://doi.org/10.3382/ps/pev252.
Yi D, Hou Y, Wang L, Ouyang W, Long M, Zhao D, et al. L-Glutamine enhances enterocyte growth via activation of the mTOR signaling pathway independently of AMPK. Amino Acids 2015;47(1):65–78. https://doi.org/10.1007/s00726-014-1842-8.
Zhang H, Wong EA. Identification of cells expressing OLFM4 and LGR5 mRNA by in situ hybridization in the yolk sac and small intestine of embryonic and early post-hatch chicks. Poultry Sci 2018;97(2):628–33. https://doi.org/10.3382/ps/pex328.
Zhang H, Wong EA. Spatial transcriptional profile of PepT1 mRNA in the yolk sac and small intestine in broiler chickens. Poultry Sci 2017;96:2871–6. https://doi.org/10.3382/ps/pex056.